An All-Dielectric Coaxial Waveguide

M. Ibanescu,[1] Y. Fink,[2] S. Fan,[1] E. L. Thomas,[2]
J. D. Joannopoulos[1]

An all-dielectric coaxial waveguide that can overcome problems of polarization rotation and pulse broadening in the transmission of optical light is presented here. It consists of a coaxial waveguiding region with a low index of refraction, bounded by two cylindrical, dielectric, multilayer, omnidirectional reflecting mirrors. The waveguide can be designed to support a single mode whose properties are very similar to the unique transverse electromagnetic mode of a traditional metallic coaxial cable. The new mode has radial symmetry and a point of zero dispersion. Moreover, because the light is not confined by total internal reflection, the waveguide can guide light around very sharp corners.

Waveguides are the backbone of modern optoelectronics and telecommunications systems. There are currently two major, and very distinct, types of waveguides (metallic and dielectric) that are used in two separate regimes of the electromagnetic spectrum. For radio frequencies, the metallic coaxial cable is of greatest prominence (*1*). In this type of cable, the entire electromagnetic field is confined between two coaxial metal cylinders. The important fundamental electromagnetic mode of a coaxial cable is the transverse electromagnetic (TEM) mode, which is unique in that it has radial symmetry in the electric field distribution and a linear relationship between frequency and wave vector. This gives the TEM mode two exceptional properties. First, the radial symmetry implies that one need not worry about possible rotations of the polarization of the field after it passes through the waveguide. Second, the linear relationship ensures that a pulse of different frequencies will retain its shape as it propagates along the waveguide. The crucial disadvantage of a coaxial metallic waveguide is that it is useless at optical wavelengths because of heavy absorption losses in the metal. For this reason, optical waveguiding is restricted to the use of dielectric materials. However, because of the differences in boundary conditions of the electromagnetic fields at metal and dielectric surfaces, it has not previously been possible to recreate a TEM-like mode with all-dielectric materials.

Consequently, optical waveguiding is done with the traditional index-guiding (that is, total internal reflection) mechanism, as exemplified by silica and chalcogenide optical fibers. Such dielectric waveguides can achieve very low losses (*2*). Although the optical fiber has proven to be undeniably successful in many ways, it is nevertheless plagued by two fundamental problems. First, because the fundamental mode in the fiber has an electric field with twofold p-like symmetry, the polarization of light coming in one end of the fiber and the polarization coming out the other are generally completely different. This leads to substantial problems when coupling into polarization-dependent devices. Second, because the guiding involves total internal reflection, it is not possible for light to travel in a fiber with a sharp bend whose radius of curvature is less than 3 mm without significant scattering losses (*3*). For light at optical wavelengths, this is a comparatively enormous radius, thus limiting the scale of possible miniaturization.

Recently, however, all-dielectric waveguides have been introduced that confine optical light by means of one-dimensional (1D) (*4*) and 2D (*5*, *6*) photonic bandgaps. Although single-mode propagation is still twofold p-like symmetric, these new designs have the potential advantage that light propagates mainly through the empty core of a hollow waveguide (*7*), thus minimizing effects associated with material nonlinearities and absorption losses. Moreover, because confinement is provided by the presence of at least a partial photonic bandgap, this ensures that light should be able to be transmitted around a bend with a smaller radius of curvature than is possible with the optical fiber.

Here we introduce a waveguide, the coaxial omniguide, that combines some of the best features of the metallic coaxial cable and the dielectric waveguides. It is an all-dielectric coaxial waveguide and supports a fundamental mode that is very similar to the TEM mode of the metallic coaxial cable. It has a radially symmetric electric field distribution so that the polarization is maintained throughout propagation. It can be designed to be single-mode over a wide range of frequencies. In addition, the mode has a point of intrinsic zero dispersion around which a pulse can retain its shape during propagation, and this point of zero dispersion can be placed in the single-mode frequency window. Finally, the coaxial omniguide can be used to guide light around sharp bends whose radius of curvature can be as small as the wavelength of the light. This waveguide design is completely general and holds over a wide range of structural parameters, materials, and wavelengths. To our knowledge, this work represents the first successful attempt to bridge the disparate modal regimes of the metallic coaxial cable and the dielectric waveguides.

A cross section of a traditional metallic coaxial waveguide is shown in Fig. 1A. Light is confined in the radial direction in the region between the two metal cylinders and travels in the axial direction (perpendicular to the plane of the figure). In a simple ray model, propagation of light through the coaxial cable can be viewed as a result of successive specular reflections off the metal

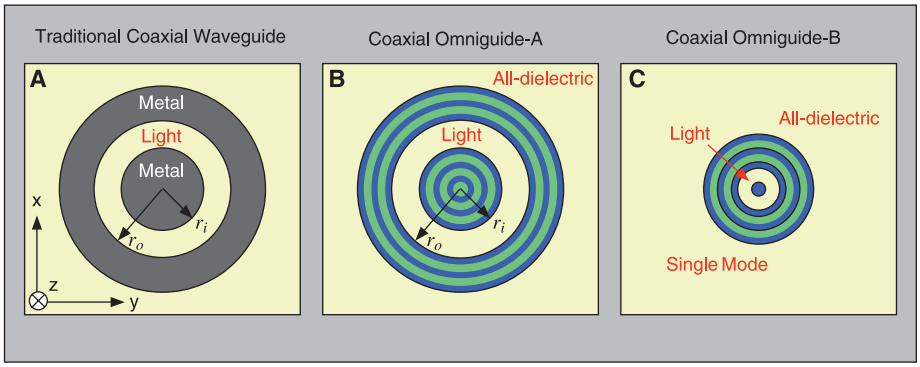

Fig. 1. Schematics of coaxial waveguide cross sections. (**A**) Traditional metallic coaxial cable. (**B** and **C**) Two embodiments, of type A and B, respectively, of the all-dielectric coaxial omniguide as described in the text. The blue cylindrical dielectric layers correspond to high dielectric constant material, and the green cylindrical dielectric layers correspond to low dielectric constant material. For all cases (A through C), light can be confined within the coaxial region (for example, $r_i < r < r_o$) and guided along the axial or *z* direction. In (A) and (B), $r_i = 3.00\ a$ and $r_o = 4.67\ a$, whereas in (C), $r_i = 0.40\ a$ and $r_o = 1.40\ a$.

[1]Center for Materials Science and Engineering and Department of Physics, Massachusetts Institute of Technology, Cambridge, MA 02139, USA. [2]Department of Materials Science and Engineering, Massachusetts Institute of Technology, Cambridge, MA 02139, USA.

walls. The dispersion relations for the first few modes supported by a metallic coaxial waveguide are shown in Fig. 2A. For definiteness, the inner and outer radii of the waveguiding region are taken to be $r_i = 3.00\ a$ and $r_o = 4.67\ a$, respectively, where a is an arbitrary unit of length to be defined later. For any value of the wave vector, the lowest frequency mode is the TEM mode for which both the electric and magnetic fields are transverse to the direction of propagation. This mode has zero angular momentum, which means that the mode is invariant under rotations around the axial direction. Another useful property of this mode is its constant group velocity, which makes it dispersionless at any frequency. The other modes shown in the plot are transverse electric (TE_{ml}) modes for $l = 1$ and varying angular momenta m (*8*). The cutoff frequency of any of these modes is of the form

$$\omega_{\text{cutoff}} = \frac{c}{r_o} f\left(\frac{r_o}{r_i}\right)$$

where f is the solution to a transcendental equation for each value of the angular momentum m and for each polarization (TE or TM) (*1*).

Designing an all-dielectric waveguide with similar principles of operation as the metallic coaxial waveguide is not straightforward, because the boundary conditions at a dielectric-dielectric interface differ from those at an air (dielectric)–metal interface. In particular, specular reflections cannot be obtained on a dielectric-dielectric interface when the ray of light comes from the region with a lower index of refraction. Thus, it has generally been assumed that an all-dielectric coaxial waveguide cannot be designed to support a TEM-like mode, even in principle. However, recent research on the omnidirectional dielectric reflector (*9*) has opened new possibilities for reflecting, confining, and guiding light with all-dielectric materials. Indeed, a dielectric hollow waveguide using this principle was recently fabricated and tested successfully at optical wavelengths (*4*). The omnidirectional dielectric reflector, or simply the dielectric mirror, is a periodic, multilayered planar structure consisting of alternating layers of low and high indices of refraction. This structure can be designed so that there is a range of frequencies at which incoming light from any direction and of any polarization is reflected. Moreover, the electric fields of the reflected light in this frequency range have corresponding phase shifts that are quite close to those acquired upon reflection from a metal. In fact, there is a frequency for each angle of incidence and each polarization, for which the phase shift is identical to that of a metal. This observation, together with the fact that high reflectivity of the omnidirectional dielectric mirror is maintained for all angles of incidence, strongly suggests exploration of the possibilities of using an omnidirectional mirror in lieu of a metal in coaxial cable designs. In effect, the omnidirectional dielectric mirror provides a new mechanism for guiding optical and infrared light without incurring the inherent losses of a metal.

In a cross section of a coaxial waveguide (Fig. 1B), the metal cylinders from the left panel have been replaced with cylindrical dielectric layers (*10*) associated with an omnidirectional mirror. We call this particular coaxial waveguide embodiment coaxial omniguide A. The parameters of the dielectric layers are taken from the hollow waveguide experiment (*4*) to be the following: Layers shown in dark blue have an index of refraction $n_1 = 4.6$ and a thickness $d_1 = 0.33\ a$, whereas layers shown in green have $n_2 = 1.6$ and $d_2 = 0.67\ a$. Here, $a = d_1 + d_2$ is the unit length of periodicity of the multilayered structure. The inner (r_i) and outer (r_o) radii of the coaxial waveguiding region are taken to be the same as those of the metallic coaxial cable described earlier. For the calculations presented here, we have set the index of refraction of the coaxial waveguiding region

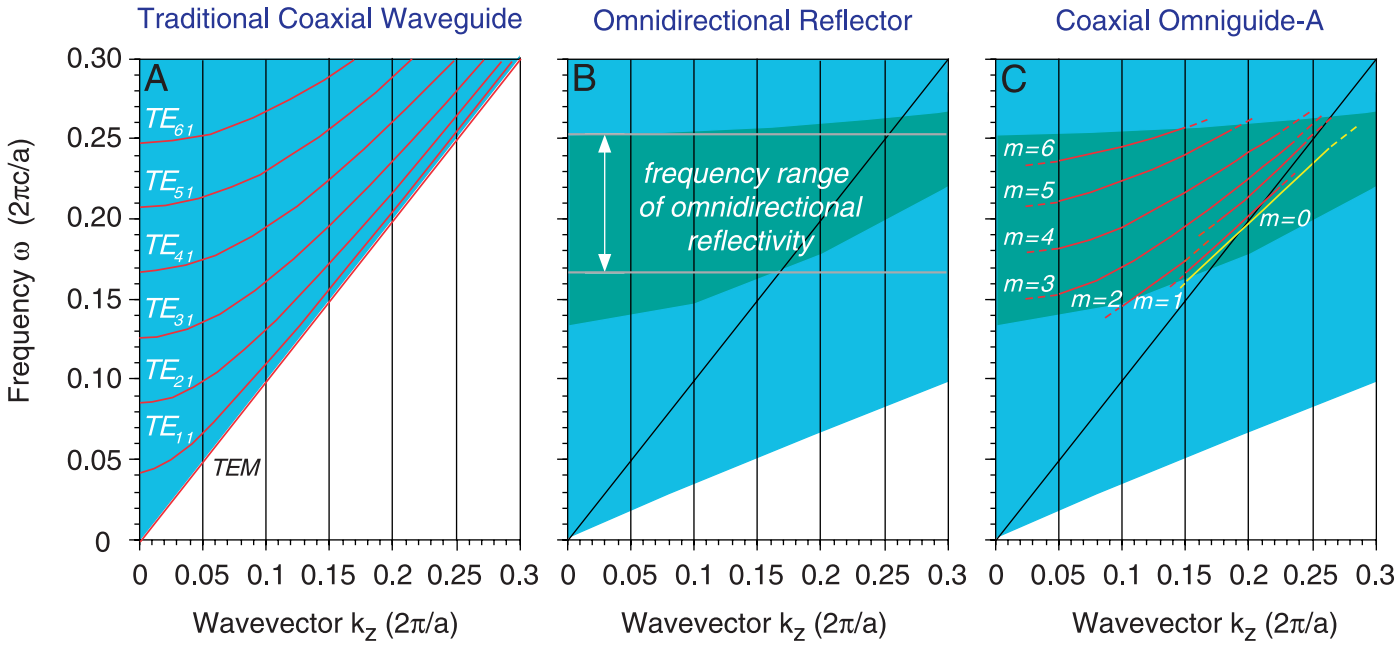

Fig. 2. Projected band structures along an axial direction. (**A**) Traditional metallic coaxial cable with inner and outer coaxial radii of $r_i = 3.00\ a$ and $r_o = 4.67\ a$, respectively. The red bands correspond to allowed guided modes. For any given wavevector, the lowest frequency mode is a TEM mode characterized by a perfectly linear dispersion relation. The six next highest bands correspond to transverse electric (TE_{ml}) modes with $l = 1$ and increasing angular momentum m. (**B**) Omnidirectional, reflecting, all-dielectric multilayer film. Light-blue regions correspond to modes for which light is allowed to propagate within the dielectric mirror, and dark-blue regions correspond to modes for which light is forbidden to propagate within the dielectric mirror. The diagonal black line identifies the edge of the light cone. The horizontal gray lines mark the boundaries in frequency within which omnidirectional reflectivity is possible. (**C**) Coaxial omniguide A with inner and outer coaxial radii of $r_i = 3.00\ a$ and $r_o = 4.67\ a$, respectively, and bilayers consisting of indexes of refraction $n_1 = 4.6$ and $n_2 = 1.6$ and thickness $d_1 = 0.33\ a$ and $d_2 = 0.67\ a$, respectively. The red and yellow bands indicate guided modes confined to the coaxial region of the waveguide. The dashed lines indicate modes with less than 20% localization within the coaxial region. There is close correspondence between the modes labeled $m = 1$ to $m = 6$ and those of (A) labeled TE_{11} to TE_{61}. Also, the yellow $m = 0$ mode corresponds to a TEM-like mode, as discussed in the text.

to be 1. In practice, in order to provide structural support, the coaxial waveguiding region may be chosen to be a dielectric with a low index of refraction without affecting the favorable properties of the coaxial omniguide (*11*).

Before we begin our investigation of the modes supported by the coaxial omniguide, it is instructive to first review the modes of a planar omnidirectional dielectric mirror. The projected band structure of the omnidirectional mirror is shown in Fig. 2B. The light blue regions represent allowed propagation modes of light within the dielectric mirror. The dark blue region represents modes for which light is forbidden to propagate within the dielectric mirror. The thick black line identifies the edge of the light cone, and the horizontal gray lines demarcate the frequency range of omnidirectional reflectivity. It is precisely within this range of frequencies that one would expect the coaxial omniguide to support modes that are most reminiscent of those of the metallic coaxial cable. To calculate the frequencies and field patterns of the modes of coaxial omniguide A, we proceed as described below.

As a result of the cylindrical symmetry of the system, there are two good "conserved quantities" that can be used to specify and classify the various modes supported by this waveguide. These are k_z, the axial component of the wave vector, and m, the angular momentum ($m = 0, 1, 2 \ldots$). For a given mode, the radial and angular components of the electric and magnetic fields can be calculated from the corresponding z (axial) components (*12*). For a given wave vector k_z and angular momentum m, the axial field components in a layer of index n have the general form

$$F(z,r,\phi) = [AJ_m(k_T r) + BY_m(k_T r)] \times (C_1 e^{im\phi} + C_2 e^{-im\phi}) e^{i(\omega t - k_z z)} \quad (1)$$

where F stands for either E_z or H_z; J_m and Y_m are Bessel functions (*13*) of the first and second kind, respectively; and k_T is a transverse wave vector $k_T = \sqrt{(n\omega/c)^2 - k_z^2}$.

The modes of the coaxial omniguide are calculated with two different approaches. The first is a semianalytic approach based on the transfer matrix method (*14*). Starting from Maxwell's equations, the z components of the electric and magnetic fields in each layer can be written in the general form given by Eq. 1. For given k_z, ω, and m, the only variables that determine the E_z and H_z fields are the four coefficients in front of the Bessel functions (two for E_z and two for H_z). The boundary conditions at the interfaces between adjacent layers can be written in the form of a matrix equation

$$\begin{pmatrix} A \\ B \\ A' \\ B' \end{pmatrix}_{j+1} = \mathbf{M} \begin{pmatrix} A \\ B \\ A' \\ B' \end{pmatrix}_{j} \quad (2)$$

where $\begin{pmatrix} A \\ B \\ A' \\ B' \end{pmatrix}_j$ are the coefficients that determine the electric and magnetic fields in the jth layer, and $\mathbf{M}$ is a 4-by-4 transfer matrix that depends on k_z, ω, m, the geometry of the layers, and their indices of refraction. After calculating the electromagnetic fields for a given point (k_z, ω), we find the resonant modes by examining the fractional E-field power confinement in the coaxial waveguiding region; that is

$$\int_{r_i < r < r_o} d\mathbf{r}\varepsilon(\mathbf{r})|\mathbf{E}(\mathbf{r})|^2\omega \Big/ \int_{\text{all layers}} d\mathbf{r}\varepsilon(\mathbf{r})|\mathbf{E}(\mathbf{r})|^2\omega \quad (3)$$

The second approach involves a numerical solution of Maxwell's equations in the frequency domain with the use of the conjugate gradient method within the supercell approximation (*15*). Supercells of size (30 a by 30 a by 0.1 a) were used, leading to a basis set of about 230,000 plane waves. Eigenvalues were considered converged when the residue was less than 10^{-6}. The results of both approaches were found to agree to better than 0.1%.

In the projected band structure for coaxial omniguide A (Fig. 2C), the red and yellow bands represent guided modes localized within the region defined by the inner and outer coaxial radii of the waveguide. The dashed lines represent modes with less than 20% localization within the coaxial region. There is close correspondence between the modes within the omnidirectional reflectivity range labeled $m = 1$ to $m = 6$ and those of the coaxial cable labeled TE_{11} to TE_{61} (*16*). The $m = 0$ mode appears to correspond to the TEM mode. Of course, for a coaxial omniguide with a limited number of outer shells, these modes can only exist as resonances. Nevertheless, even with only 2.5 bilayers, we find that they can be extremely well localized resonances, and the leakage rate decreases exponentially with the number of shells. The strong localization is shown in Fig. 3. Here, we plot the power density in the electric field for the four lowest frequency modes at $k_z = 0.19\ (2\pi/a)$. As the color bar indicates, power increases in going from black to dark red, to red, to orange, to yellow. The blue circles identify the boundaries between the various dielectric shells and are included as a guide to the eye. In all cases, the power is confined primarily within the coaxial region. This is particularly true for the $m = 0$ mode, which is also cylindrically symmetric, just like the TEM mode. Although it is well known that a waveguide consisting only of dielectric material cannot support a true TEM mode (*17*),

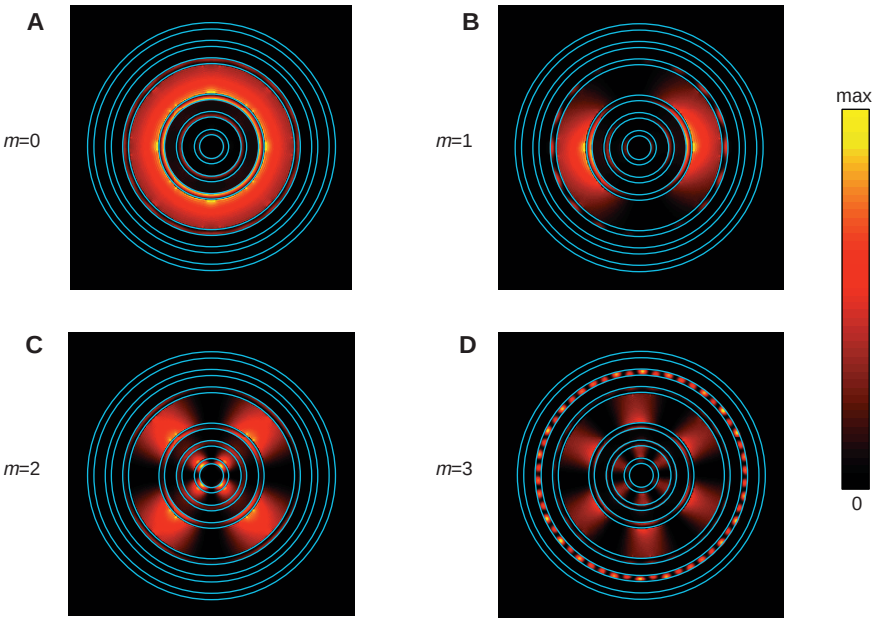

Fig. 3. Power density in the electric field for guided modes at $k_z = 0.19\ (2\pi/a)$ in Fig. 2C. (**A** through **D**) correspond to guided modes with angular momenta $m = 0$ to $m = 3$, respectively. The color bar indicates that power increases in going from black to dark red, to red, to orange, to yellow. The blue circles identify the boundaries between the various dielectric shells and are included as a guide to the eye. Most of the power is confined to the coaxial region of the waveguide. The cylindrical symmetry and radial dependence of the $m = 0$ mode are consistent with those of a TEM mode. [The small fluctuations in density away from perfect cylindrical symmetry in (A) are a consequence of the discrete cubic grid used in the computations.]

we find that the $m = 0$ mode (which is a pure TM mode) possesses several of the characteristics of the TEM mode. First, as mentioned above, it has zero angular momentum and hence a radially symmetric electric field distribution. Second, the electric and magnetic fields within the coaxial waveguiding region (where over 65% of the power is concentrated) are nearly identical to those of the metallic coaxial cable; for example, the predominant components are E_r and H_f and vary as $1/r$. Finally, at the point where the $m = 0$ dispersion curve (yellow line) crosses the light line, there is an exact correspondence between the electromagnetic fields of the coaxial omniguide and the metallic coaxial cable, inside the coaxial region. Moreover, the derivative of the group velocity is exactly zero near this point, leading to nearly dispersionless propagation throughout its vicinity (*18*).

The characteristics described above are certainly the attributes one would hope to achieve in order to overcome problems with polarization-rotation and pulse broadening. But what about single-mode behavior? The bands shown in Fig. 2C are clearly multimode; that is, for a given frequency there are two or more guided modes that can be excited. To design a coaxial omniguide that can support single-mode behavior, we need only readjust our structural parameters. It is easier to keep the parameters of the bilayers fixed, so that the omnidirectional reflectivity frequency range does not change. This leaves only those parameters that are common to both the coaxial omniguide and the metallic coaxial cable: the inner and outer radii of the coaxial waveguiding region. Single-mode operation for the TEM-like mode will only be possible if all other modes are moved up in frequency so that the lowest nonzero angular mode has its cutoff frequency inside the bandgap. To do this, we have to decrease the inner radius of the coaxial waveguiding region. At the same time, the thickness of the bilayers, a, should remain constant, which means that we can no longer accommodate three bilayers in the inner part of the waveguide. Actually, the inner radius has to be decreased so much that we are forced to discard the periodic structure in the inner region and to replace it with a single dielectric rod. Loss of the inner-core mirror structure is not crucial, however. What is important is to add a thin rod of dielectric in the core in order to avoid the $1/r$ divergence of the field at the origin and to use a dielectric of high enough contrast to localize the TEM-like mode in the coaxial region. This approach, however, will not work if $r_i > a$, and one must then revert to a multilayer core. Testing different values for the inner and outer radii of the waveguiding region, we have found a configuration that has the desired properties. This new embodiment, coaxial omniguide B, is shown in Fig. 1C. The central dielectric rod has an index of refraction $n_1 = 4.6$ and a radius $r_i = 0.40\ a$. The coaxial waveguiding region has an outer radius $r_o = 1.40\ a$, and the parameters of the outer bilayers are the same as those used for configuration A. In configuration B, there are two frequency ranges where the waveguide can operate in a single-mode fashion. We plot the dispersion curves for the modes supported by coaxial omniguide B in Fig. 4. The yellow dots indicate more than 50% confinement of the electric field power, whereas the red dots represent confinement between 20 and 50%. (The dashed lines indicate confinement that is less than 20%.) The two white boxes identify the frequency ranges where the $m = 0$ band is single-mode. A comparison of Figs. 2C and 4 reveals that the cutoff frequency of the $m = 1$ band has shifted significantly upward, whereas the $m = 0$ band remains relatively unchanged. The flatness of the $m = 1$ band (*19*) enables the TEM-like band to be single-mode both above it and below it in frequency. The exact values of the parameters were chosen so that, in the middle of the higher frequency single-mode window [at $\omega = 0.205\ (2\pi c/a)$], the mode is also dispersionless (*18*).

Figure 5 shows the distribution of the electric field components for the $m = 0$ mode of coaxial omniguide B at $k_z = 0.2\ (2\pi/a)$ and $\omega = 0.203\ (2\pi c/a)$. Because the (k_z, ω) point is very close to the light line, the electric field in the waveguiding region is almost completely transverse to the direction of propagation. (The z component of the magnetic field will always be zero because this is a pure TM mode.) The field distribution clearly reveals a high confinement of the mode in the waveguiding region, as desired. Moreover, these values of E_x and E_y lead to a net field distribution that is completely radially symmetric, consistent with an angular component that is exactly zero. All the features mentioned above attest to the close correspondence between the $m = 0$ mode and a pure TEM mode.

There are several additional issues associated with the coaxial omniguide. The first is a practical issue involving the coupling of light into the coaxial omniguide. One possible method for coupling would be to begin with an omniguide with a very thin core that increases gradually to match the core of the coaxial configuration. Because the electromagnetic field of a laser source can have a TEM_{00} mode, this should lead to efficient coupling into the TEM-

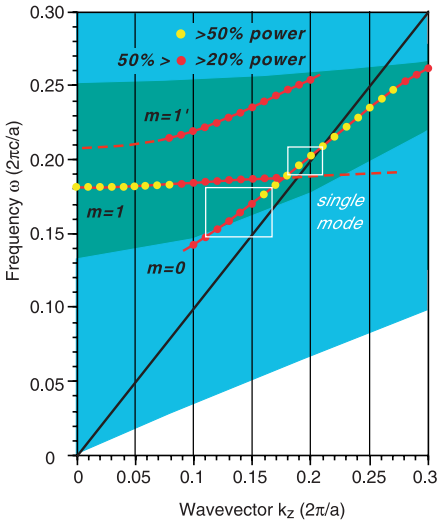

Fig. 4. Projected band structure for coaxial omniguide B. The central dielectric rod has an index of refraction $n_1 = 4.6$ and a radius $r_i = 0.40\ a$. The coaxial waveguiding region has an outer radius $r_o = 1.40\ a$, and the parameters of the outer bilayers are the same as those used for configuration A. The yellow dots represent confinement of the electric field power of more than 50%; the red dots represent confinement between 20 and 50%; and the dashed lines represent confinement less than 20%. The two white boxes identify the frequency ranges where the $m = 0$ band exhibits single-mode behavior.

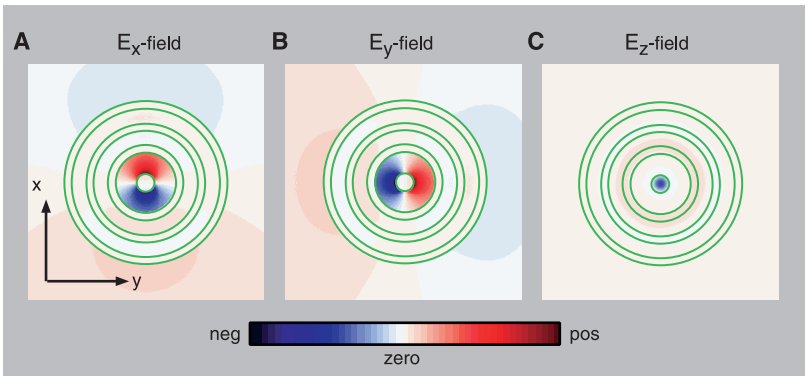

Fig. 5. Electric field for the mode at frequency $0.203\ (2\pi c/a)$ and $k_z = 0.2\ (2\pi/a)$ in Fig. 4. (**A** through **C**) Electric field components along the x, y, and z directions, respectively. The color bar indicates that large positive and negative values are shown as dark red and dark blue regions, respectively, whereas white areas represent regions of zero values of the electric field, and light-colored areas represent regions of low values of the electric field. The field distribution clearly reveals a high confinement of the mode in the coaxial waveguiding region, and in this region it is nearly completely transverse to the direction of propagation (less than 10^{-3} of the intensity is along z), as desired.

like mode of the coaxial omniguide. The second issue concerns the ability to transmit information across a broad band of frequencies with the coaxial omniguide. This is determined primarily by the width of the omnidirectional reflectivity range. Another issue is that the multitude of adjustable parameters in the structure of a coaxial omniguide (the index of refraction and thickness of each layer, the thickness of a bilayer, the waveguiding region inner and outer radii, the central rod index of refraction, and so on) allows for great flexibility in tuning the waveguide for optimal desired performance (confinement in the waveguiding region, width of single-mode window, frequency of zero dispersion, group velocity, and so on). A further important issue is that radial confinement of the light is a consequence of omnidirectional reflection and not of total internal reflection. This means that the coaxial omniguide can be used to transmit light around much sharper corners than is possible with the optical fiber. Finally, the radial decay of the electromagnetic field in the coaxial omniguide is much faster than in the case of the optical fiber (with only 10 bilayers, one gets a decrease of electric field intensity of about six orders of magnitude). This means that, for guided light of the same wavelength, the outer diameter of the coaxial omniguide can be much smaller than the diameter of the cladding layer of the optical fiber without leading to cross-talk complications in waveguide bundles. These enabling characteristics of a substantially smaller waveguide bending radius and smaller spacing of adjacent waveguides lead to the possibility of substantial miniaturization of future integrated optical devices and transmission lines.

References and Notes

1. R. A. Waldron, *Theory of Guided Electromagnetic Waves* (Van Nostrand Reinhold, London, 1969).
2. B. E. A. Saleh and M. C. Teich, *Fundamentals of Photonics* (Wiley, New York, 1991).
3. See, for example, S. E. Miller and A. G. Chynoweth, Eds., *Optical Fiber Telecommunications* (Academic Press, New York, 1979).
4. Y. Fink *et al*., *J. Lightwave Technol.* **17**, 2039 (1999).
5. J. C. Knight *et al.*, *Science* **282**, 1476 (1998).
6. R. F. Cregan *et al*., *Science* **285**, 1537 (1999).
7. The first attempts at hollow waveguides in the optical regime actually involved metallodielectric materials. See, for example, M. Miyagi *et al.*, *Appl. Phys. Lett.* **43**, 430 (1983), and Y. Matsuura and J. Harrington, *J. Opt. Soc. Am.* **14**, 6 (1997), and references therein.
8. The waveguide also supports transverse magnetic (TM) modes, but they do not appear in the plot because the cutoff frequency for the lowest lying TM mode is larger than 0.30 ($2\pi c/a$).
9. Y. Fink *et al*., *Science* **282**, 1679 (1998).
10. The idea of radially confining light by means of a dielectric multilayer structure was first investigated by P. Yeh *et al.* (*14*). Our work differs in that our waveguide is coaxial, and the multilayer film is chosen so that there exists a frequency range of omnidirectional reflectivity. Both of these properties are important in order to create a TEM-like mode.
11. For example, setting the index of refraction of the coaxial waveguiding region to 1.3 (instead of 1.0), with $n_1 = 4.6$ and $n_2 = 1.8$, the original omnidirectional reflectivity frequency range of 0.17 to 0.25 ($2\pi c/a$) in Fig. 2B reduces to a range of 0.18 to 0.23 ($2\pi c/a$), whereas the modal structure shown in Fig. 2C remains essentially unaltered.
12. A. Yariv, *Optical Electronics in Modern Communications* (Oxford Univ. Press, New York, 1997).
13. C. J. Tranter, *Bessel Functions with Some Physical Applications* (Hart, New York, 1969).
14. P. Yeh, A. Yariv, E. Marom, *J. Opt. Soc. Am.* **68**, 1196 (1978).
15. R. D. Meade *et al.*, *Phys. Rev. B* **77**, 8434 (1993); erratum: *Phys. Rev. B* **55**, 15942 (1997).
16. The small discontinuity in $m = 2$ arises from a weak coupling to a resonant mode of the same symmetry localized deep within the core region.
17. N. J. Cronin, *Microwave and Optical Waveguides* (Institute of Physics, Bristol, UK, 1995).
18. For simplicity, we only consider the intrinsic waveguide dispersion in all our calculations. In a real waveguide, we would also have material dispersion, which can be compensated for in the standard manner by judicious tuning of the waveguide parameters. Indeed, the multitude of available parameters for the coaxial omniguide provides a much greater flexibility to accomplish this than in the case of an optical fiber.
19. We find that the very small group velocity exhibited by the $m = 1$ mode can be driven even to negative values with a proper choice of waveguide parameters.

20. We thank S. Johnson for many helpful discussions. Supported in part by the U.S. Army Research Office under grant DAAG55-97-1-0366, by the Materials Research Science and Engineering Center of NSF under award DMR-9808941, and by the U.S. Department of Energy under grant DE-FG02-99ER45778.

20 March 2000; accepted 25 May 2000

Holes in a Quantum Spin Liquid

Guangyong Xu,[1] G. Aeppli,[2] M. E. Bisher,[2] C. Broholm,[1,3]* J. F. DiTusa,[4] C. D. Frost,[5] T. Ito,[6] K. Oka,[6] R. L. Paul,[3] H. Takagi,[7] M. M. J. Treacy[2]

Magnetic neutron scattering provides evidence for nucleation of antiferromagnetic droplets around impurities in a doped nickel oxide–based quantum magnet. The undoped parent compound contains a spin liquid with a cooperative singlet ground state and a gap in the magnetic excitation spectrum. Calcium doping creates excitations below the gap with an incommensurate structure factor. We show that weakly interacting antiferromagnetic droplets with a central phase shift of π and a size controlled by the correlation length of the quantum liquid can account for the data. The experiment provides a quantitative impression of the magnetic polarization cloud associated with holes in a doped transition metal oxide.

Spin density modulations in transition metal oxides are receiving huge attention because of possible connections to high-temperature superconductivity. The modulations appear upon introduction of charge carriers, through chemical substitution, into an insulating and antiferromagnetic parent compound and tend to be static when the carriers are frozen and dynamic when they are mobile. Evidence for such modulations has been largely confined to materials whose magnetism and charge transport are quasi–two-dimensional (*1–4*) and whose parent insulators are ordered antiferromagnets. We provide evidence for analogous phenomena in a quasi–one-dimensional oxide (*5*), $Y_{2-x}Ca_xBaNiO_5$, for which the parent is a spin liquid by virtue of quantum fluctuations (*6–10*) and which has motivated considerable theoretical activity (*11–16*).

The key features of this orthorhombic material are the chains of NiO_6 octahedra (Fig. 1A). The octahedra are corner-sharing, which results in the dominance of magnetism (*8*) and electrical conduction (*5*) by the very simple ..O-Ni-O-Ni-O.. backbone. The magnetic degree of freedom at each Ni site is the spin $S = 1$ associated with the $3d^8$ configuration of Ni^{2+}. Each of the $S = 1$ ions is coupled to its neighbors through antiferromagnetic (AFM) superexchange through shared O^{2-} ions. Replacing the off-chain Y^{3+} by Ca^{2+} introduces holes primarily onto apical oxygen atoms in the chains, and while the materials remain insulators, doping substantially increases conductivity at finite temperatures. Thus, $Y_{2-x}Ca_xBaNiO_5$ is a one-dimensional analog of the cuprates, where off–CuO_2-plane chemical impurities donate holes to the CuO_2 planes.

Magnetic one-dimensionality causes the parent compound Y_2BaNiO_5 to be a spin liquid prevented from ordering antiferromagnetically by quantum fluctuations. The material is not an ordinary paramagnet with heavily damped spin fluctuations, but rather the magnetic analog of superfluid ^{4}He because it has a macroscopically coherent quantum

[1]Department of Physics and Astronomy, Johns Hopkins University, Baltimore, MD 21218, USA. [2]NEC Research Institute, 4 Independence Way, Princeton, NJ 08540, USA. [3]National Institute of Standards and Technology Center for Neutron Research, Gaithersburg, MD 20899, USA. [4]Department of Physics and Astronomy, Louisiana State University, Baton Rouge, LA 70803, USA. [5]ISIS Facility, Rutherford Appleton Laboratory, Chilton, Didcot, Oxon OX11 0QX, UK. [6]Electrotechnical Laboratory, Tsukuba 305, Japan. [7]Department of Advanced Materials Science, Graduate School of Frontier Sciences, University of Tokyo Hongo, Tokyo 113-8656, Japan.

*To whom correspondence should be addressed. E-mail: broholm@jhu.edu